Available online at www.sciencedirect.com

ScienceDirect

Energy Procedia 77 (2015) 29 – 35

Energy Procedia

5th International Conference on Silicon Photovoltaics, SiliconPV 2015

Soft breakdown behavior of interdigitated-back-contact silicon solar cells

Haifeng Chu*, Lejo J. Koduvelikulathu, Valentin D. Mihailetchi, Giuseppe Galbiati, Andreas Halm, Radovan Kopecek

ISC Konstanz e.V., Rudolf-Diesel-Str. 15, 78467, Konstanz, Germany

Abstract

The soft reverse IV characteristic of interdigitated-back-contact (IBC) silicon solar cells consisting of contiguous p^+ and n^+ regions on the rear side (Figure 1) was investigated in this study. Our IBC cell concept, which is a 6-inch IBC cell with a diffused phosphorous BSF and a boron front floating emitter, features a relatively low breakdown voltage of about - 3.7 V. We measured a negative temperature coefficient at reverse bias in the dark. The low breakdown voltage and the negative temperature coefficient both support the hypothesis that the high reverse current is caused by the tunneling effect [1]. We demonstrated that by changing the doping profiles, the breakdown voltage of the IBC cells can be modified. Our simulations show that the reverse bias current is mainly caused by the band-to-band tunneling across the borders of the p^+ and n^+ regions, and that the breakdown voltage changes with doping profiles. Furthermore, a qualitative agreement is found between the experimental and simulated reverse currents. In principle, the same theory may apply for studying the early breakdown behavior of MWT, EWT or any other cells that feature p^+n^+ junctions.

Peer review by the scientific conference committee of SiliconPV 2015 under responsibility of PSE AG

Keywords: Silicon solar cell, IBC, breakdown voltage, band-to-band tunneling

* Corresponding author. Tel.: +49 (0) 7531 / 36 183 - 371; fax: +49 (0) 7531 / 36 183 - 11
E-mail address: haifeng.chu@isc-konstanz.de

Peer review by the scientific conference committee of SiliconPV 2015 under responsibility of PSE AG
doi:10.1016/j.egypro.2015.07.006

1. Introduction and advantages of soft breakdown

The IBC cell concept has captured considerable attention thanks to its potential to achieve high efficiency. For IBC cells that consist of contiguous p^+ and n^+ regions on the rear side (Figure 1), a soft reverse IV characteristic has been observed [2-4]. The reverse breakdown of this type of cells usually takes place at a low breakdown voltage Vr ($|Vr| < 5$ V), and more importantly, it is non-destructive and uniform over the entire cell.

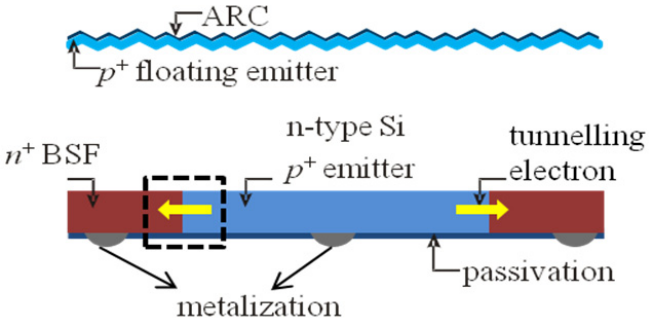

Fig. 1. IBC cells with contiguous p^+ and n^+ regions on the rear side.

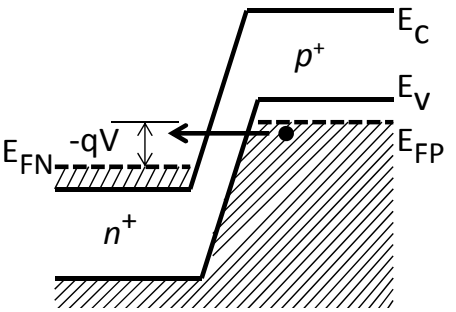

Fig. 2. Energy-band diagram of a heavily doped p^+n^+ junction at reverse bias. (Adapted from [1])

In stark contrast, the breakdown of standard front-contact solar cells usually takes place at a high voltage ($|Vr| >$ 10 V) and at one or several local breakdown sites, where the overwhelming current might lead to non-reversible damage to the cell. Therefore bypass diodes are introduced to the module to prevent the front-contact cells from being operating at a high reverse voltage. But once the bypass diode is turned on, the power generated by the other cells from the same string is wasted.

As for IBC cells that feature soft breakdown, partial or complete shadowing of one cell does not necessarily turn on the bypass diode and therefore the energy yield of the PV system could be increased. In addition, a cell with a lower breakdown voltage is preferred, because when it is shadowed, it would consume less power generated from the illuminated cells [2, 3, 5].

In this paper we firstly studied the cause of the soft breakdown and verified it for our IBC cells by measurement. Secondly we fabricated IBC cells with different doping profiles, which led to different breakdown voltages. Simulation study was also performed to model the band-to-band tunneling effect that is responsible for the soft breakdown.

2. Cause of the soft breakdown

2.1. Theory

Figure 2 shows that when a highly doped p^+n^+ junction is reverse biased, electrons can tunnel from the valence band into the conduction band. The tunneling current follows

$$J_t \propto AFV \exp(-B/F) , \quad (1)$$

where F is the average electric field inside the junction, V is the applied voltage, A and B are positive quantities that are related to material properties, such as the band gap and the effective mass of carriers [1]. Hence a higher electric field shall lead to a higher tunneling current. The same phenomenon may occur in IBC cells, if the doping concentration of the p^+ emitter and n^+ BSF is heavy enough to enable the tunneling current. This tunneling current could lead to the desired soft breakdown characteristic [2, 3, 6].

2.2. Breakdown mechanism: tunneling effect

We fabricated IBC cells on 6 inches n-type Cz-Si wafers with a thickness of about 190 μm and a base resistivity of 3.9 Ω·cm. A simplified schematic cross-section of our cells is shown in Figure 1. The front floating emitter, rear emitter and BSF were all formed by diffusion. The interdigitated pattern on the rear side was achieved by laser structuring with a Rofin laser system. For more details of cell processing please refer to [7]. For the study in this section we selected a cell with the following performance under AM 1.5 spectrum and 25 °C: Voc=652 mV, Jsc=39.8 mA/cm^2, FF=80.5 %, and η=20.9 % respectively. As depicted in Figure 3, this cell shows a soft breakdown characteristic, with a breakdown voltage V_r of about - 3.7 V. Note that the breakdown voltage V_r is defined as the voltage at which the reverse current reaches 2 A, which corresponds to a current density of 8.4 mA/cm^2. This definition belongs to one of the many definitions of breakdown voltage summarized in [8] and it is used throughout this paper.

A common method to distinguish between avalanche multiplication and tunneling is to measure the temperature coefficient. The former breakdown mechanism has a positive temperature coefficient and a high breakdown voltage ($|V_r|$ > 6.7 V for Si), while the latter has a negative temperature coefficient and a low breakdown voltage ($|V_r|$ < 4.5 V for Si) [1]. To verify whether the current is mainly caused by the tunneling effect, we measured the revere bias dark IV curves at 26 °C and 104 °C. The results are shown in Figure 3. One can find that for a given reverse voltage, the absolute value of the reverse current increases with temperature, when the reverse current is over 0.7 A (or |reverse voltage| > 2.5 V). Therefore this cell has a negative temperature coefficient in this current range. The negative temperature coefficient and the low breakdown voltage of about - 3.7 V both support the hypothesis that the breakdown current is caused by the tunneling effect.

The reverse bias electroluminescence (ReBEL) image of the same cell (Figure 4) shows relatively uniform and high EL signal along all the parallel borders between the p^+ and n^+ regions. This implies that the high tunneling current flows through all the p^+n^+ junctions, instead of crowding into several local spots. This uniform breakdown over the entire junction area results in uniform heat dissipation when the cell is reverse biased in the module, and thus significantly reduces the risk of damaging the cell and the module. No degradation is found on the cell efficiency after the reverse bias measurements. A rigorous test of continuous biasing our cells at - 10 A showed only 0.1 % drop in efficiency [4]. This feature shows the potential of applying the soft breakdown characteristic in the field (the shadowed case) with our cells.

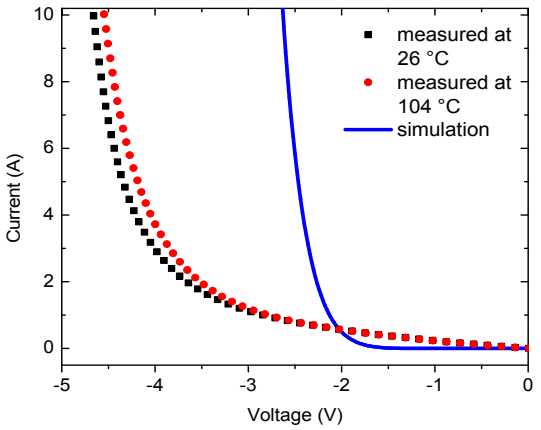

Fig. 3. Measured reverse IV curves at 26 °C and 104 °C.

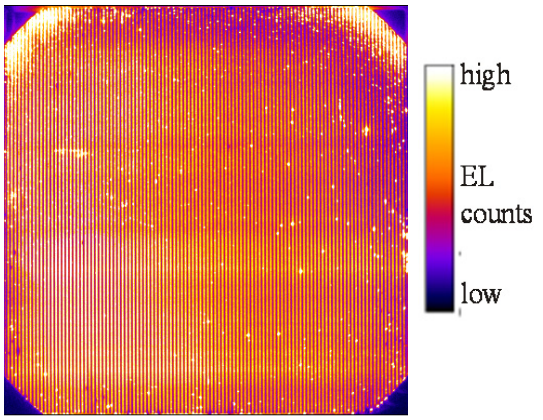

Fig. 4. ReBEL image of the IBC cell in Fig. 3 biased at - 4.7 V and with – 10.2 A flowing.

The part with weaker EL signal in Figure 4 may be resulted from lighter doping concentration there, which may be caused by the slight non-uniformity in the diffusion process. In order to verify this hypothesis, we intentionally

performed an inhomogeneous boron diffusion. One monitor wafer was placed next to the cell precursor during the phosphorous diffusion, while the other during the boron diffusion. Figure 5 and 6 show the sheet resistance maps of these two monitor wafers measured by the junction photovoltage (JPV) method. One can find that the phosphorous diffusion is quite homogeneous, while the boron diffusion is not. The upper-center part of the wafer features higher sheet resistance. Interestingly, this inhomogeneity is reflected in the ReBEL image of the cell (Figure 7), where weaker ReBEL signal is found. Hence the doping concentration has an impact on the ReBEL signal. Uniform diffusions shall lead to homogeneous ReBEL images.

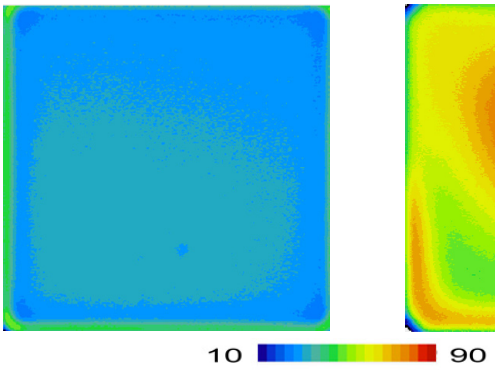

Fig. 5. Rsh map of phosphorous diffusion on the monitor wafer.

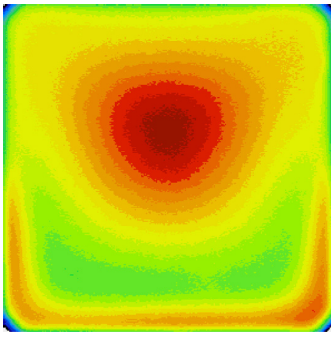

Fig. 6. Rsh map of boron diffusion on the monitor wafer.

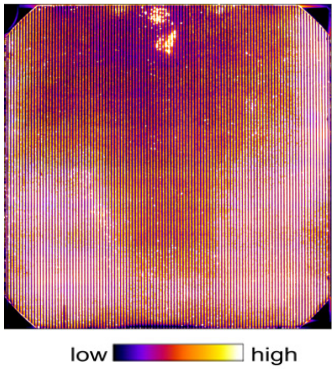

Fig. 7. IBC cell with inhomogeneous ReBEL signal, biased at - 4.5 V and with -9.8 A flowing.

3. Experiment: modifying the breakdown voltage

Following the idea that the doping profiles are key factors that decide the breakdown voltage, we fabricated IBC cells with different combinations of phosphorous and boron doping profiles. Table 1 summarizes the sheet resistances of each group. Figure 8 and 9 show the ECV measurement profiles of the boron and phosphorous diffusions used in this experiment. Apart from the doping profiles, all the other fabrication processes were kept the same. The results shown in Figure 3 and 4 in section 2.2 come from group 4.

Table 1. Experimental groups with different doping profiles. Breakdown voltage is defined as the voltage at which the reverse current reaches 2 A.

Group	1	2	3	4	5
Boron sheet resistance (Ohm/sq)	51	63	63	78	127
Phosphorous sheet resistance (Ohm/sq)	18	25	90	19	90
Breakdown voltage (V)	- 2.9	- 4.2	- 4.6	- 3.7	- 5.1
pFF (%)	76.6	79.3	82.1	81.4	79.7
Efficiency (%)	17.3	19.7	21.4	20.9	20.0

Figure 10 depicts the measured reverse IV curves of each group measured at 25 ± 2 °C, whereas Figure 11 shows the relation between the breakdown voltage and the boron and phosphorous sheet resistances. Generally the breakdown voltage increases with sheet resistances. However, the doping concentration and depth of the boron and phosphorous diffusions, together with the lateral interdiffusion between the emitter and BSF, decide the electrical

properties of the p^+n^+ junction, and hence the breakdown voltage [6]. The last two rows of Table 1 list the pseudo fill factor (pFF) and best cell efficiency of each group. Surface passivation and screen-printed metallization of all investigated groups are not optimized yet and they are considered to be the main causes of recombination. So far no clear relation is found between the breakdown voltage and pFF, or between the breakdown voltage and efficiency. Based on the relatively high pFF, the cells are at least not expected to be shunted. We demonstrated that by changing the doping profiles, one can modify the breakdown voltage of IBC cells.

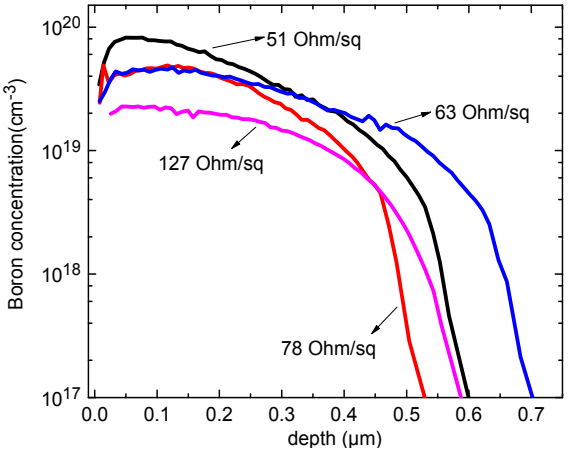

Fig. 8. Boron doping profiles used in the experiment.

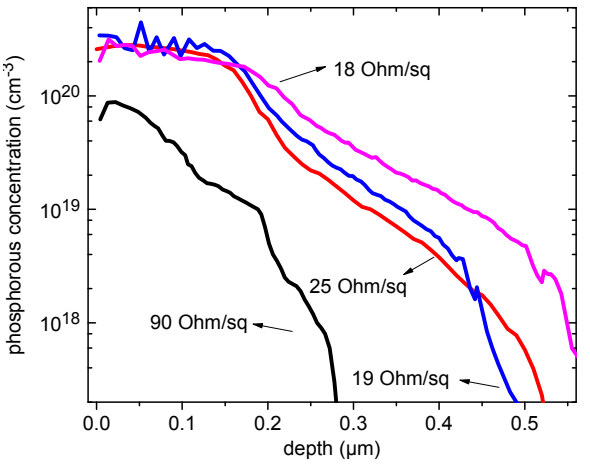

Fig. 9. Phosphorous doping profiles used in the experiment.

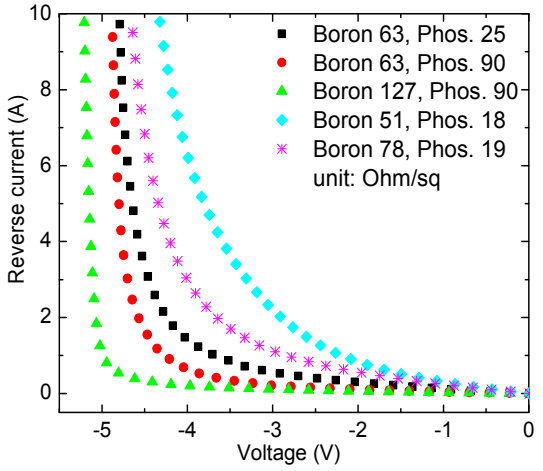

Fig. 10. Measured reverse IV curves from groups listed in Table 1.

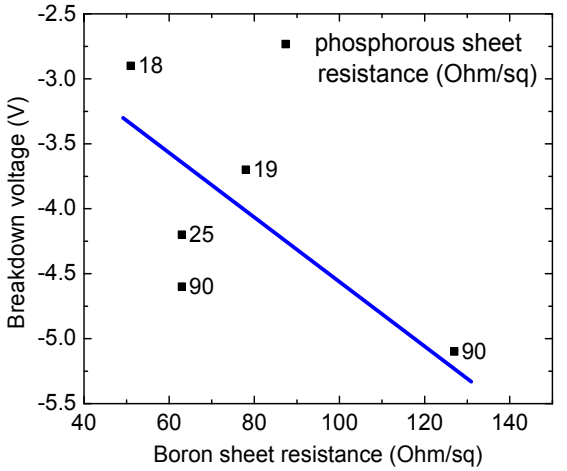

Fig. 11. Breakdown voltage changes with doping profiles.

4. Simulation of the reverse tunneling current

4.1. simulation of one p^+n^+ junction

We performed simulation by ATLAS, SILVACO TCAD suite [9] to study the reverse bias breakdown mechanisms. The band-to-band (BTB) tunneling current is the dominant current at reverse bias and therefore we included it in our simulation [2]. The model structure is similar to the one highlighted by the black frame in

Figure 1. However, a slightly modified model structure was used in the simulation to consider the actual cell structure. In order to save computational time, we did not calculate the entire unit cell, rather only the part near the border of the p^+ emitter and the n^+ BSF, an area of 1 μm ×1 μm. We expected nearly all the tunneling current to flow over this small interface area. To obtain satisfactory accuracy, a very fine mesh with a minimum spacing of 0.3 nm along the tunneling direction was set. The experimental ECV profiles of p^+ emitter and n^+ BSF were loaded for the simulation study. Figure 12 shows that, in reverse bias the BTB tunneling current far outweighs the saturation current, and thus the reverse current is mainly dominated by the tunneling current.

4.2. Simulation of the entire solar cell

In order to make a direct comparison between the experiment and the simulation, the simulated tunneling current from the model structure (results from Figure 12) was scaled to estimate the total tunneling current in the cell by means of multiplying the full length of the cell and the number of p^+n^+ junctions. This method is valid as long as the reverse current generated over the p^+n^+ junction is nearly identical to the reverse current generated over one unit cell, and it is confirmed by our simulation. In this way a large amount of calculation time is saved. The simulated reverse current of the entire solar cell of group 4 is depicted in Figure 3, where one can observe qualitative agreement between the experimental and simulated data.

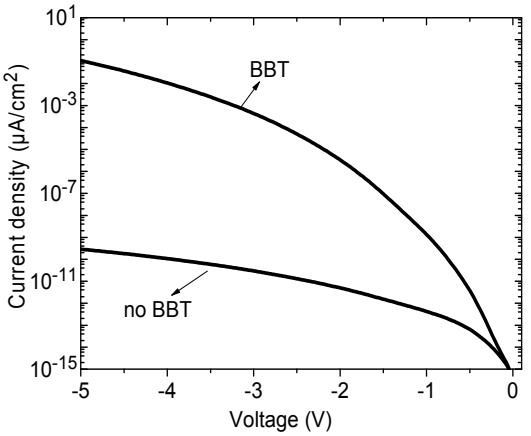

Fig. 12. Simulated IV curves at reverse bias with and without the band-to-band (BTB) tunneling model.

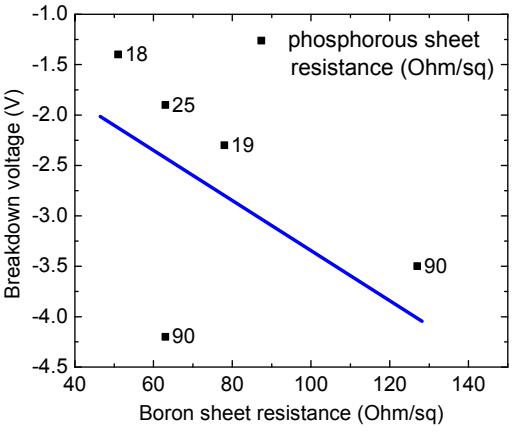

Fig. 13. Simulated reverse breakdown voltages of groups listed in Table 1.

Figure 13 plots the simulated reverse breakdown voltages of all groups listed in Table 1. Based on the results from Figure 11 and 13, we find that overall the simulation can predict the tendency regarding the change of breakdown voltage with doping profiles. However, the simulated breakdown voltages are smaller than the experimental ones. From Figure 13, a higher phosphorous or boron sheet resistance is required in the simulation to attain the experimental breakdown voltage. The mismatch between simulation and experiment might derive from the lack of knowledge of the actual doping profiles in the finished cell near the border of the p^+ and n^+ regions, or from other unknown factors that are not taken into account yet. Still, the mature theory that was developed for the tunnel diode seems to be valid for the IBC cell as well.

5. Conclusions and outlook

The soft breakdown characteristic in IBC cells with contiguous emitters and BSFs was observed. Based on the relatively low breakdown at about - 3.7 V and the negative temperature coefficient, the soft breakdown probably results from the band-to-band tunneling effect. The system yield could be enhanced thanks to the uniform and soft breakdown characteristic.

We demonstrated that by changing the doping profiles, the breakdown voltage of the IBC cells can be modified. Numerical simulation with the use of the theory of band-to-band tunneling model shows that at reverse bias condition, the tunneling current is dominant, as compared to the reverse bias saturation current. In addition, the simulation is able to achieve a qualitative agreement with the measured reverse IV curves. Further research is needed to gain a better modeling of the reverse current, to understand the correlation between the breakdown voltage and other factors, such as pFF and efficiency, and to fabricate cells with high efficiency and lower breakdown voltage. Before making use of the soft breakdown characteristic in the field, a long degradation test at reverse bias, e.g. for hundreds of hours, is necessary to check whether the cell experiences serious degradation.

In principle, the same theory and strategy of modifying breakdown voltage could be used to study the early breakdown behavior of MWT, EWT or any other cells that feature p^+n^+ junction [10, 11].

Acknowledgements

The authors would like to thank Rafael Peyronnet-Dremiere for the support of fabrication and measurements. This work was funded by the project HERCULES which has received funding from the European Union's Seventh Programme for research, technological development and demonstration under the grant agreement No 608498.

References

[1] S. M. Sze, K. K. Ng, "Physics of semiconductor devices", 3rd ed, New Jersey: Wiley, 2007.
[2] K. Mangersnes, S.E. Foss, "Tunneling in back-junction silicon solar cells", in: Proceedings of the 28th European PV Solar Energy Conference, Paris, France, 2013.
[3] D. D. Smith et al., "Generation III high efficiency lower cost technology: transition to full scale manufacturing", in: Proceedings of the 38th IEEE Photovoltaic Specialists Conference, Austin, TX, USA, 2012.
[4] A. Halm et al., "The zebra cell concept - large area n-type interdigitated back contact solar cells and one-cell modules fabricated using standard industrial processing equipment", in: Proceedings of the 27th European PV Solar Energy Conference, Frankfurt, Germany, 2012.
[5] A. M. Gabor et al., "Solar panel design factors to reduce the impact of cracked cells and the tendency for crack propagation", in: NREL PV Module Reliability Workshop, Denver, USA, 2015.
[6] U. Römer et al., "Counterdoping with patterned ion implantation", in: 39th IEEE Photovoltaic Specialists Conference, Tampa, Florida, USA, 2013.
[7] G. Galbiati et al., "Large-area back-contact back-junction solar cells with efficiency exceeding 21%", in: Proceedings of the 38th IEEE Photovoltaic Specialists Conference, Austin, TX, USA, 2012.
[8] S. Mahadevan et al., "Electrical breakdown in semiconductors", physica status solidi (a) 8.2, 1971: 335-374.
[9] ATLAS User's manual, Device simulation software, SILVACO, 2014.
[10] B. Geerligs, "Progress in n-type MWT technology", in: 5th MWT Workshop, Freiburg, Germany, 2013.
[11] F. Kiefer, et al. "High efficiency n-type emitter-wrap-through silicon solar cells", Photovoltaics, IEEE Journal of 1.1, 2011: 49-53.